A Four-Fermi Model in 0+1 Dimensions in Matter

Romuald A. Janik[a], Maciej A. Nowak[a], Gábor Papp[b] and Ismail Zahed[c]

[a]Department of Physics, Jagellonian University, 30-059 Krakow, Poland.

[b]Institut für Theor. Physik, Univ. Heidelberg, Philosophenweg 19, D-69120 Germany

[c]Department of Physics and Astronomy, SUNY, Stony Brook, New York 11794, USA.

The results of a number of constituent quark models in matter may be understood in the mean-field approximation by using a simple four-fermi model in 0+1 dimensions.

1. Introduction

The fate of the spontaneous breaking of chiral symmetry in matter is still stirring a broad interest in light of present and future heavy-ion collision experiments. Most of our understanding of the issue from first principles is limited to finite temperature, where lattice simulations have been carried out [1]. At finite chemical potential, present Monte-Carlo algorithms are upset by the complex character of the measure [2].

A number of past and present analyses of the subject relies on QCD inspired models, such as the instanton model [3,4], or variants of the NJL model [5]. A common feature to all these models, is the the emergence of chiral constituent quarks in the vacuum, following the spontaneous breaking of chiral symmetry. These models do not confine.

The purpose of this talk is to show that the underlying mechanisms at work in most of these models can be captured using a four-fermi model in 0+1 dimensions [4]. In section 1, we review the model in the presence of chiral scalar and vector interactions. In section 2 we analyze its schematic thermodynamical content. In section 3, we construct the quark condensate and discuss its relation to the scalar quark content of the constituent quark at low densities. In section 4, we construct the resolvent and the distribution of eigenvalues for the present model in the quenched approximation. In section 5, we derive the spectral sum rules for the present model in the quenched and unquenched approximation. Our conclusions are given in section 6.

2. Model

Consider a quark field $\psi_{a,f}$ where $a = 1, 2, ..., N$ are 'color' indices, and $f = 1, 2, ..., N_f$ are flavor indices. For simplicity $N_f = 1$ unless specified otherwise. By analogy with NJL models, the Lagrangian density is chosen to be [6]

$$
\begin{aligned}
\mathcal{L}_1 &= \psi^\dagger(i\gamma_4\partial_4 + im + i\mu\gamma_4)\psi \\
&+ \frac{g^2}{2}\left((\psi^\dagger\psi)^2 + (\psi^\dagger i\gamma_5\psi)^2\right) + g_\omega^2(\psi^\dagger i\gamma_4\psi)^2
\end{aligned}
\tag{1}
$$

or equivalently

$$
\begin{aligned}
\mathcal{L}_1 &= R^\dagger i(\partial_4 + (\mu - \omega_4))L + \frac{1}{2g^2}PP^\dagger - \frac{1}{4g_\omega^2}\omega_4^2 \\
&+ L^\dagger i(\partial_4 + (\mu - \omega_4))R \\
&+ R^\dagger i(P + m)R + L^\dagger i(P^\dagger + m)L\,.
\end{aligned}
\tag{2}
$$

The model will be discussed on a circle of radius $\beta = 1/T$ in one dimension unless specified otherwise. The gamma matrices are chosen such that $\gamma_4 = \text{offdiag}(1,1)$ and $\gamma_5 = \text{diag}(1,-1)$, in the chiral basis with $\psi = (R, L)$. The auxiliary fields are: $P = -2ig^2 L^\dagger L$, $P^\dagger = -2ig^2 R^\dagger R$ and $\omega_4 = -2g_\omega^2 \psi^\dagger i\gamma_4 \psi$.

For $m = 0$ (chiral limit), the model exhibits massive (constituent) quark excitations at low densities, and massless (free) quark excitations at high densities in the limit $N \to \infty$ (mean-field). In the same limit, qq, qqq, $\bar{q}q$, ... phases and/or exitations are down by $1/N$. Although the model lacks confinement, it bears much in common with more realistic chiral constituent quark models such as the instanton or the NJL model [4]. For an analysis of the thermodynamics in a confining model we refer to [7].

3. Thermodynamics

On a circle with boundary condition $\psi(\tau + \beta) = -\psi(\tau)$, the operator $i\partial_4$ is invertible with a discrete spectrum $\omega_n = (2n + 1)\pi T$. In the mean-field approximation or large N, the pressure per particle associated to (1-2) for $N_f = 1$ is [4,6]

$$
\frac{1}{\mathbf{n}}p = \omega - T\log(1 - n)(1 - \overline{n}) - \Sigma PP^\dagger + \alpha \omega_4 \omega_4^\dagger
\tag{3}
$$

with the usual occupancies $n, \bar{n} = 1/(1 + \exp((\omega \mp (\mu - \omega_4))/T))$. Here $\omega = |P + m|$, $\Sigma = V_3/2g^2$ and $\alpha = V_3/g_\omega^2$, following the rescaling $\psi \to \sqrt{V_3}\psi$. The thermodynamical limit will be carried with $N \to \infty$ at fixed $\mathbf{n} = N/V_3$. (3) describes a quark with two energy levels $\pm \omega$ at finite temperature and chemical potential. The first term is the 'zero point' motion, and the last two terms are exchange contributions [6]. The gap equations are

$$
2\Sigma P = 1 - n - \bar{n}\,, \quad \rho = \mathbf{n}(n - \bar{n}) = 2\alpha \mathbf{n}\,\omega_4\,.
\tag{4}
$$

(4) admit several solutions of which the one with maximum pressure will be selected. Generically there are two phases: a broken phase with constituent quarks and a symmetric phase with free quarks. For $\alpha < \Sigma$ there is a μ region with no real solutions to (4). In the symmetric phase the pressure is $p = \mathbf{n}(\mu - 1/4\alpha)$, while in the broken phase it is $p = \mathbf{n}/4\Sigma$, for $m = T = 0$. The phase change occurs at $\mu_c = 1/4\Sigma + 1/4\alpha$.

For $\alpha = \infty$ (vanishing vector coupling) the model is that used originally by us [6] and others [8]. In the broken phase $P_* = 1/2\Sigma$ for $\rho = 0$ with the pressure $p = \mathbf{n}(m + 1/4\Sigma)$. In the symmetric phase $P_* = 0$ for $\rho = \mathbf{n}$ and $p = \mathbf{n}\mu$. The phase changes are mean-field driven and can be analyzed at the critical points using universality arguments [6]. For any m there is a first order transition at $\mu_* = (m + 1/4\Sigma)$ [4,6].
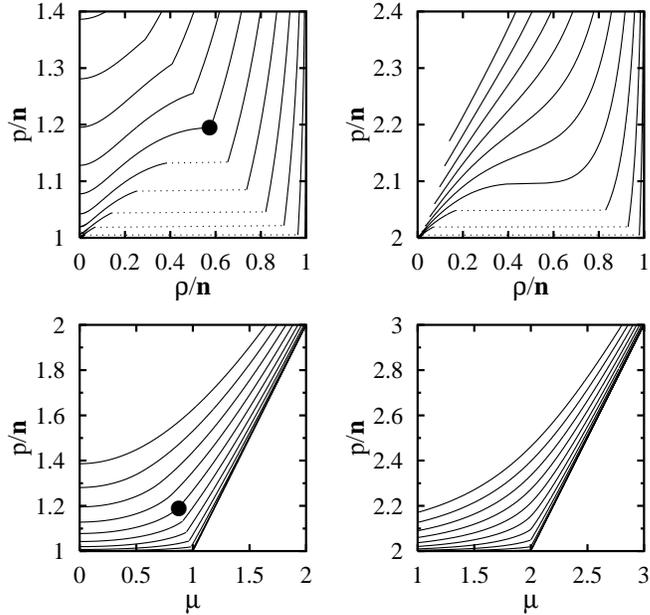
Figure 1. Isotherms at $m = 0$ (left) and $m = 1$ (right).

The occurrence of a first order transition for small values of the temperature for light current masses is not generic to constituent quark models. Indeed, in NJL models the first order transition in the chiral limit is usually turned to a cross-over transition for light quark masses [5]. The cross-over is robust against parameter changes in the presence of a vector interaction. The first order transition observed in these models at $T = 0$ is much like the one studied in Walecka-type models in the form of a liquid-gas transition at low nucleonic matter density [9]. In the latter, the nucleon mass is the constituent mass and $m = 0$.

In Fig. 1 we show the isotherms in temperature steps of $\Delta T = 1/2$ for $m = 0$ (left) and $m = 1$ (right), with $\Sigma = 1$. At low temperature the transition is first order with a jump in the density (Maxwell construction) turning into a second order transition at high temperature. This is in agreement with our original arguments [4,6], and more recent investigations [10]. With increasing mass the 'tricritical' point shifts down to lower temperatures, and the second order transition is turned to a cross-over. This confirms what is usually observed in NJL type models: a first order transition in the massless case and a cross-over in the presence of light quarks [5].

4. Quark Condensate

The behavior of the quark condensate $|\langle \overline{q}q \rangle| = 2\mathbf{n}\,\Sigma m_Q$ with $m_Q = P_*$ and $m = 0$ is shown in Fig. 2 as a function of temperature and density in the chiral limit. The solid line is the phase boundary crossing the tricritical point (big dot) beyond wich a mixed phase is developing. The hole in the middle reflects on the mixed phase. The size of the hole shrinks with increasing mass m, making it closer in shape to the result obtained in NJL type models in 4 dimensions [5]. Above the tricritical point $T_{3c} = m_Q/3$ and $\rho_{3c} = \mathbf{n}/\sqrt{3}$
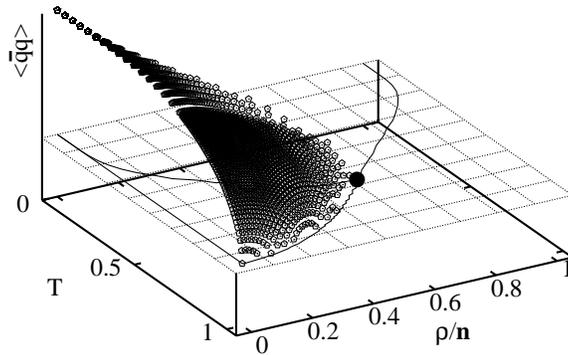
4

Figure 2. $|\langle \overline{q}q \rangle|$ in the $T\rho$ plane. See text.

or $\mu_{3c} = m_Q \log(2+\sqrt{3})/3$, the transition is first order and disappears at $\mu_* = m_Q/2$. At $\mu = 0$, the transition is second order (mean-field) and sets in at $T_* = m_Q/2$. Amusingly, for a constituent mass $m_Q \sim 300$ MeV, $\mu_* = T_* \sim 150$ MeV, and $\mu_{3c} \sim T_{3c} \sim 100$ MeV. In the absence of matter, $\mathbf{n} = |\langle \overline{q}q \rangle| \sim (200 \text{ MeV})^3$. Hence $\rho_{3c}/\rho_0 \sim 10/3$ where $\rho_0 = 0.17$ fm^{-3} is nuclear matter density. Most of these numbers are similar to the ones observed in NJL models [5].

The slope of the chiral condensate for small densities carries information on the 'pion-nucleon' σ term. Here the role of the nucleons is played by constituent quarks. For small temperature the slope is -1 at the origin and reflects on the scalar charge of the constituent quark. This is to be compared to -2.5 from the 2-flavour pion-nucleon sigma term with $\sigma_0 \sim 40$ MeV and a current mass $m \sim 8$ MeV.

5. Quark Spectrum

For $\alpha = \infty$, the pseudoscalar four-Fermi interaction in (1) causes the quarks to interact as if they were moving in a random Gaussian potential provided by the new auxiliary fields $\mathcal{A}_{ab}(\tau) \sim \psi_a \psi_b^\dagger(\tau)$ which is an $N \times N$ complex valued function of τ[4,6]. For fixed $\mathcal{A}$, the quark spectrum follows from

$$\gamma_4(i\partial_4 + \mathcal{A} + i\mu)\psi^k = \lambda_k[\mathcal{A}]\,\psi^k \qquad (5)$$

with anti-periodic boundary conditions and

$$2\mathcal{A} = \mathbf{A}\,(1+\gamma_5) + \mathbf{A}^\dagger\,(1-\gamma_5). \qquad (6)$$

which is symmetric, complex and block-off-diagonal. (5) in the present model is the analogue of the QCD eigenvalue equation in external gauge field. The Gaussian averaging with moments

$$\left\langle \mathcal{A}_{ab}\mathcal{A}_{cd}^\dagger \right\rangle_{\mathcal{A}} = \frac{1}{2N\Sigma}\delta_{ac}\delta_{bd} \qquad (7)$$

restores the four-fermi interaction. The spectrum (in the $n = 0$ sector for $\mathcal{A}$ symmetric) can be readily probed through the distribution of eigenvalues

$$\varrho(z,\overline{z}) = \frac{1}{N}\sum_k \left\langle \delta(z - \lambda_k[\mathcal{A}]) \right\rangle_{\mathcal{A}} \qquad (8)$$
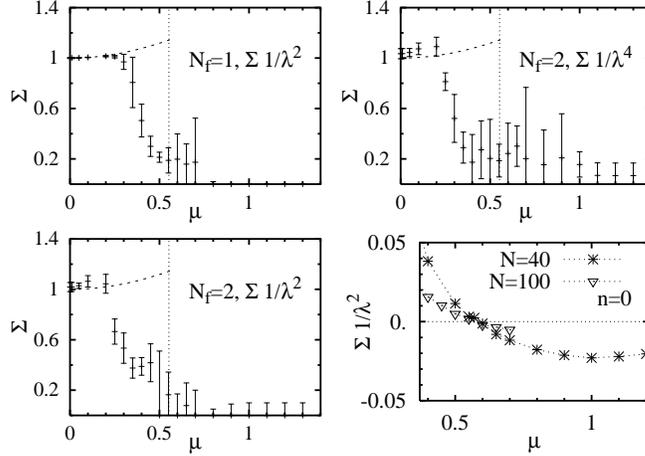
Figure 3. Spectral sum rules. See text.

which is complex valued for finite μ. Setting $T = 0$ in (3) the model dimensionally reduces to a 0+0 dimension one which is a matrix model.

The quenched distribution (8) can be easily constructed [11,12]. For small values of μ the density of eigenvalues concentrates near the imaginary axis, while for large values it does not. The unquenched distribution of eigenvalues is harder to generate (complex weight induced by quark feedback). However, we expect qualitatively a similar behavior but with a finite accumulation of eigenvalues on the real axis. The chiral transition from finite density to zero set in at intermediate values of μ for which the density of eigenvalues along the real axis would vanish in the thermodynamical limit $N \to \infty$. To characterize the onset of the transition quantitatively we suggest to use the microscopic sum rules as we now show.

6. Spectral Sum Rules

For fixed N_f, the spectral sum rule for our case reads

$$\frac{1}{N^2}\Big\langle\Big\langle \sideset{}{'}\sum_k \frac{1}{\lambda_k^2[\mathcal{A}]} \Big\rangle\Big\rangle_0 = \frac{\langle q^\dagger q \rangle^2}{2N_f} = \frac{1}{2N_f}\left(\frac{\partial p}{\partial m}\right)^2 \tag{9}$$

where the averaging is over the matrices $\mathcal{A}$ with the unquenched measure in the 0+0 model (no Matsubara modes). The sum rule (9) allows for a determination of the chiral condensate (low density). Near $\mu \sim \mu_*$ the finite size corrections are important, upsetting the present construction. In Fig. 3 the chiral condensate extracted from (9) in the 0+0 model (averaged over 5×10^5 matrices) is shown for one (upper left) and two (lower left) flavours. In the upper right corner we show the chiral condensate extracted from the next sum rule. The dashed lines indicate the analytical result of the condensate. The lower right corner shows the sum rule (9) for the quenched ($N_F = 0$) case and *finite N* (for $N \to \infty$ (9) diverges). Due to the elongation of the support of eigenvalues for large chemical potential, the sum rule changes sign. The numerical analysis indicates that this change occurs around the critical chemical potential ($\mu_* \approx 0.5277$ [11]). This suggests

that the quenched physics may still 'remember' the unquenched one at the critical point, through the way the complex eigenvalues in (8) get redistributed near zero.

7. Conclusions

We have constructed a chiral four fermi model with the thermodynamical structure of a two-level quark system. This model undergoes first and second order-type transitions, and can be used to illustrate how the quark spectrum may be probed in matter. We used this model to show that the microscopic spectral sum rules are sensitive to temperature and chemical potential changes including a phase transition in the unquenched approximation. The interplay between the thermodynamical limit, the chiral limit, the quenched-unquenched approximations and the precision of numerical algorithms are readily addressed in this model. We believe the present analysis to be useful for current lattice QCD simulations with matter.

8. Acknowledgments

REFERENCES

1. C. Detar, hep-ph/9504325; and references therein.
2. J.B. Kogut, M.P. Lombardo and D.K. Sinclair, Phys. Rev. **D51** (1995) 1282.
3. D. Diakonov, hep-ph/9602375; T. Schäfer and E.V. Shuryak, Rev.Mod.Phys. **70** (1998) 323.
4. M. Nowak, M. Rho and I. Zahed, 'Chiral Nuclear Dynamics', World Scientific 1996; and references therein.
5. for a review see U. Vogel and W. Weise, Prog. Part. and Nucl. Phys. **27** (1991) 195; S.P. Klevansky, Rev. Mod. Phys. **64** (1992) 649; M.K. Volkov, Phys. Part. Nucl. **24** (1993) 35; T. Hatsuda and T. Kunihiro, Phys. Rep. **247** (1994) 221.
6. R.A. Janik, M.A. Nowak and I. Zahed, Phys. Lett. **B392** (1997) 155; R.A. Janik, M. A. Nowak, G. Papp and I. Zahed, Acta Phys. Pol. **B27** (1996) 3271 and Acta Physica Polonica **B28** (1997) 2949.
7. T. Hansson and I. Zahed, Phys. Lett. **B309** (1993) 385, and references therein.
8. T. Wettig, T. Guhr, A. Schäfer and H. Weidenmüller, hep-ph/9701387.
9. J. Kapusta, 'Finite-Temperature Field Theory', Eds. Landshoff et al., Camb. 1989, and references therein.
10. J. Berges and K. Rajagopal, hep-ph/9804233; M.A. Halasz et al., hep-ph/9804290.
11. M. Stephanov, Phys. Rev. Lett. **76** (1996) 4472.
12. R.A. Janik, M.A. Nowak, G. Papp and I. Zahed, Phys. Rev. Lett. **77** (1996) 4876.